WARSAW UNIVERSITY OF TECHNOLOGY Index 351733
FACULTY OF CIVIL ENGINEERING
COMMITTEE FOR CIVIL AND WATER ENGINEERING
POLISH ACADEMY OF SCIENCES ISSN 1230-2945

DOI: 10.24425/ace.2026.157472

ARCHIVES OF CIVIL ENGINEERING

Vol. LXXII ISSUE 1 2026

pp. 255–269

Research paper

Study on tunnel support stability considering rock mass expansion effect in fault fracture zone

Lizhi Cheng[1], Zhiquan Yang[2], Ping Zhao[3], Yajun Liu[4], Fengting Li[5]

Abstract: This study explores a variety of mountain settlements and stress-strain problems caused by tunnels passing through mountain fault zones. Based on the research background of the Lianfeng Mountain tunnel project, the expansion pressure of the rock mass was introduced through the Kastner formula using ABAQUS finite element simulation software. A mountain structure model was established, and the structural stress state of the mountain after tunnel excavation and the stability law of the secondary lining were studied. The results showed that for the double-layer steel frame, the inner steel frame of the tunnel bore more stress. In the normal section, the settlement of the tunnel vault was similar to the amount of bottom uplift. However, in the broken section, the settlement of the vault was significantly greater than the amount of bottom uplift. The excavation of the second tunnel during the construction of the double tunnel caused the strain in the first tunnel to increase. This study provides a theoretical reference for the safety analysis of similar mountain tunnels.

Keywords: tunneling, parallel double tunnels, crushing zones, expansion pressure, numerical simulation

[1]PhD., Faculty of Public Safety and Emergency Management, Kunming University of Science and Technology, Kunming 650093, China, e-mail: lifengting_123@163.com, ORCID: 0009-0009-7191-1411
[2]Prof., PhD., Faculty of Public Safety and Emergency Management, Kunming University of Science and Technology, Kunming 650093, China, e-mail: 1025394655@qq.com, ORCID: 0009-0003-8113-0965
[3]PhD., Shandong Provincial Communications Planning and Design Institute Group Co., Ltd., Jinan 250000, China, e-mail: 2606764807@qq.com, ORCID: 0009-0008-7001-5650
[4]PhD., School of Civil Engineering, Shandong University, Jinan, e-mail: lyj96529@163.com, ORCID: 0009-0004-0965-6708
[5]MSc., School of Civil Engineering, Shandong University, Jinan, e-mail: 1062381066@qq.com, ORCID: 0000-0001-8857-0806

1. Introduction

At present, the tunnel is a key infrastructure in the fields of transportation, water conservancy, and energy and is widely used in complex geological conditions such as mountainous areas, underground rivers, and broken rock masses [1, 2]. However, tunnel engineering through the mountain fracture zone needs to face complex geological conditions, such as the geological phenomenon of serious rock separation and fragmentation in the fracture zone, which leads to the deformation and destruction of the rock mass, increasing the difficulty and risk of tunnel construction. Researchers have conducted extensive research to address these issues.

Researchers, such as Yuan Hao, have used numerical calculation models of multiple tunnels to study the deformation law of multiple tunnels crossing the mountain fracture zone [3]. Li et al. used the gray cusp mutation theory and the SSAGELM intelligent model to evaluate the current status and trend of surrounding rock stability [4]. Based on the discontinuous boundary element method of fault force displacement and discontinuity, Ma et al. simulated the formation of secondary faults and analyzed the failure law of tunnels under the influence of fracture zones [5]. Meng Lubo et al. studied the influencing factors of asymmetric and large deformations in high geostress layered soft rock tunnels using a large amount of data, which provided a method for classification and discrimination [6]. Zhang et al. used three-factor and four-level orthogonal numerical simulation experiments to analyze the sensitivity of surrounding rocks [7]. Chen et al. analyzed the collapse characteristics and mechanism of a tunnel fault fracture zone under rainfall conditions through the failure theory of the surrounding rock, three-dimensional discrete element numerical simulations, and on-site deformation monitoring [8]. Zhang et al. formulated a support scheme based on the geological engineering conditions of a roadway and used FLAC3D to simulate the stability evolution of the surrounding rock under the fault fracture zone [9]. Zheng et al. studied the deformation mode of a submarine tunnel crossing a fault zone under high water pressure and used three-dimensional finite element calculations and analyses to evaluate the effectiveness of different pre-reinforcement measures [10]. Li Zhaozhong used a genetic algorithm and a support vector machine algorithm to establish an inversion model of the surrounding rock parameters of a high-speed rail tunnel and obtained the mechanical parameters of the surrounding rock of the tunnel fault section through the inversion of actual monitoring data [11]. To clarify the pressure mechanism of the surrounding rock of a deep soft rock tunnel, based on the Milin Tunnel Project and the elastoplastic mechanics of the rock mass, Tao Qi deduced an analytical formula for the surrounding rock expansion pressure and obtained a reasonably large deformation treatment scheme [12].

In summary, the surrounding rock of the tunnel crossing the fault fracture zone is easily deformed and unstable; however, there are few studies on the support effect and deformation law of the tunnel crossing the fault fracture zone under the action of a deeply buried high geostress. Therefore, this study relies on the Lianfeng Tunnel of the Dayong Expressway in Yunnan Province to cross the fault fracture zone and uses numerical calculation and analysis methods to study the stability characteristics of the tunnel crossing the fault fracture zone under the action of high geostress to provide important construction guidance for a tunnel project to cross the fault fracture zone safely.

2. Engineering background

The section from Gaoqiao to Huanghua on the Daguan-Yongshan Expressway is located in Zhaotong City in the northeast of Yunnan Province, at the junction of Yunnan and Sichuan provinces, and in the hinterland of Wumeng Mountain. One of the key projects, the Lianfeng Tunnel, is located in Mohan Township and Lianfeng Town in Yongshan County, Zhaotong City, Yunnan Province. The tunnel is designed as a separate double-hole tunnel, with a height limit of 5 m and a width of 10.25 m. The proposed tunnel is distributed in a nearly straight linear shape, and the overall axis direction of the tunnel is about 309°. The starting and ending stations of the left line tunnel are ZK20+600~ZK31+584 with a total length of 10984 m and a slope of –2.600%, which is a long highway tunnel, with a maximum buried depth of about 732 m, located at K33+240, and the starting and ending stations of the right line tunnel are K20+583~K31+578, with a total length of 10995 m and a slope of –2.600%, which is a long road tunnel with a maximum buried depth of about 748 m, located at K33+190. The Lianfeng Tunnel mainly passes through the two wings and axes of the Laozhai oblique direction. The outlet is located on the south and east sides of the Lianfeng fault zone, and the tunnel section passes through two secondary fault fracture zones formed by the Lianfeng broom-like gyratory structure, which is derived from the Lianfeng fault. Schematic diagram of Lianfeng Mountain orientation is shown in Figure 1 below.

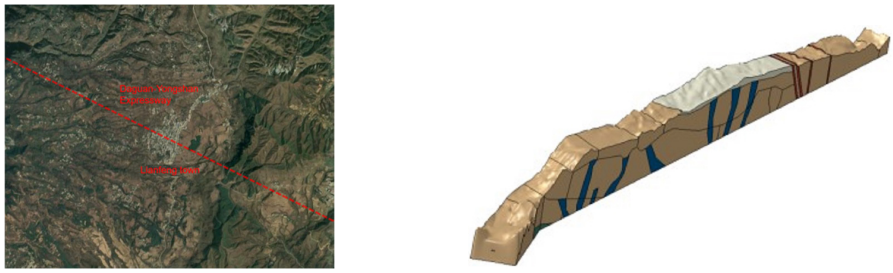

(a) (b)

Fig. 1. Schematic diagram of Lianfeng Mountain

3. Theory of cavern pressure

3.1. In-situ stress calculation

In tunnelling and rock engineering, the stability of circular caverns (tunnels and mines) is crucial. To understand the magnitude of the original in situ stress of the tunnel, Zhu Huanchun obtained the relationship between the magnitude of the in situ stress and the depth of the general rock mass by testing a large number of rocks and regression calculation mathematical models [13]. As shown in Eq. (3.1), because the rock mass involved in this study in the Dayong tunnel project is basalt with different degrees of weathering, basalt, as an eruptive rock, belongs

to the category of igneous rocks. The general in situ stress calculation formula of igneous rocks in the literature can be cited, as shown in Eq. (3.2).

$$\sigma_H = KH + T + \varepsilon \tag{3.1}$$

$$\sigma_H = 0.03311H + 13.65 \tag{3.2}$$

where K and T are the regression coefficients to be determined, H is the depth, the unit m, represents the horizontal principal stress, and the unit MPa, represents the fitting residual. The mountain construction drawings show that the average buried depth of the tunnel under Lianfeng Mountain through the fracture zone is approximately 450 m, and the in situ stress at this depth was calculated to be 28.55 MPa.

3.2. Expansion pressure calculation

The rock around the cavern is subjected to pressure and stress; therefore, it is important to investigate the magnitude of the stress around the cavern to assess its stability and safety. Kastner's formula is a classical formula used to describe the stress distribution around the perimeter of a circular cavern, considering the elastic modulus and Poisson's ratio of the rock. It provides an approximate calculation of the stress around the cavern, and it is particularly suitable for analyzing cavern stability in rock mechanics and underground engineering [14]. This formula is expressed as follows:

$$p_i = \frac{1}{\delta^2 - 1}\left[2p_0\left(\delta - 1\right) + 2\sigma_c\right]\left(\frac{R_0}{R_P}\right)^{\delta - 1} - \frac{2\sigma_c}{\delta - 1} \tag{3.3}$$

where $\delta = \dfrac{1 + \sin\varphi}{1 - \sin\varphi}$ is the friction angle in the rock body, P_0 is the initial in-situ stress, R_0 is the tunnel excavation radius, R_P is the plastic zone radius, and σ_c is the saturated uniaxial compressive strength of the rock.

According to the Geological Survey Report of Lianfeng Mountain, the internal friction angle and uniaxial compressive strength of the weathered basalt and tectonic breccia can be known, and the cavern stresses are calculated to be 53.2 MPa and 16.7 MPa, respectively. The in situ stress parameters of the two rocks are listed in Table 1.

Table 1. In-situ stress parameters of rock mass

The name of the project	Internal friction angle/(°) φ	Initial in-situ stress/(MPa)	Saturated uniaxial compressive strength/(MPa)	Cavern stress/(MPa)
Moderately weathered basalt	28	28.55	75.3	53.2
Tectonic breccia	22	28.55	26.8	16.7

4. Numerical calculation models and analytical methods

4.1. Numerical calculation model

Based on the construction drawings of the construction section of the fracture zone of the Lianfeng Tunnel, a numerical model of the construction mechanics of the Lianfeng Mountain Tunnel was constructed using the large-scale finite-element software ABAQUS, as shown in Figure 2. The model intercepts two adjacent high-risk fracture zones (480 m wide, 850 m long, and 450 m high) on the mountain with two crushing bandwidths of 67 m and 48 m, 73 m spacing, and a 61° inclination angle. To improve the quality of the grid, the tunnel part is simplified into a circular tunnel with a diameter of 7.2 m, in which the spacing between the two tunnels is 40 m, the thickness of the lining structure is 0.7 m, and the supporting structure establishes two circumferential steel frame supports inside and outside according to the tunnel reinforcement diagram, and different steel frame spacing is set up for simulation. The interaction mode of the steel frame with the lining structure is embedded. The mesh used for the model was C3D8R. The model is divided into 133952 cells and 141639 nodes.

To simulate the stress around the tunnel cavern, different stresses were applied on the normal section and outside the crushing zone lining structure, and the surface of the lining structure was vertically oriented inward. A simulation diagram of the cavern stress and the steel frame is shown in Figure 3.

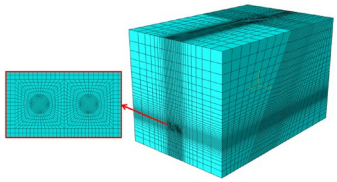

Fig. 2. Numerical calculation model

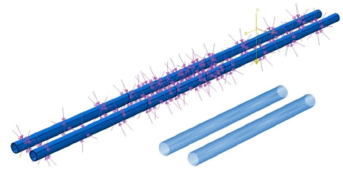

Fig. 3. Cavern stress and steel frame

The Mohr–Coulomb model was used for the entire Lianfeng Mountain, and the entire rock mass of the mountain was medium-weathered basalt. The rock mass in the fractured area was tectonic breccia, the linear elastic model was used for the lining structure, and the strength was simulated as C30 concrete. Table 2 lists the numerically calculated mechanical parameters of the model.

Table 2. Calculation parameters of the model

The name of the project	**Density/ (kg/m^3)**	**Elastic modulus/ (GPa)**	**Poisson's ratio**	**Cohesion/ (kPa)**	**Internal friction angle/ (°) φ**
Moderately weathered basalt	2760	42.4	0.17	1000	28
Tectonic breccia	2660	10.3	0.23	100	22
C30 concrete	2360	30.0	0.15	–	–
Steel frame	7850	200.0	0.30	–	–

4.2. Numerical calculation and analysis methods

The first step is the initialization of the model in-situ stress. The in-situ stress equilibrium refers to the stress state obtained by the mountain under the action of self-weight stress without considering tunnel excavation; that is, the original state before mountain excavation is restored.

The second step is tunnel excavation simulation. The element life and death method in ABAQUS is used to define the left tunnel excavation unit as a dead element.

The third step is tunnel support simulation. Using the element life and death method in ABAQUS, activate and define the left tunnel support unit, make it a living element, and modify the mechanical parameters of the support unit.

The fourth step is tunnel excavation simulation. Define the right tunnel excavation unit as a dead unit to simulate the tunnel excavation process;

The fifth step is tunnel support simulation. Activate and define the right tunnel support unit, make it a living unit, and modify the support structure model and mechanical parameters to simulate the tunnel support process.

4.3. Reliability analysis

During tunnel excavation, it is difficult to monitor the results of the interaction between the tunnel lining structure and surrounding rock mass in real-time. Therefore, to verify the accuracy of the model, an analytical solution fitting method was used in this study. Einstein and Schwartz proposed a well-known internal force solution for tunnel support systems that assumes that the rock or soil mass is an isotropic elastic homogeneous medium and is particularly suitable for circular tunnels with better accuracy for both tunnel excavation and support. Therefore, in this study, the calculated axial force of the analytical solution was compared with the axial force of the numerical simulation, and the reliability of the numerical simulation results was analyzed.

The Einstein and Schwartz equation is as follows:

$$T = \frac{PR}{2}\left\{(1+K)(1-a_0^*) + (1-K)\left[1+2a_2^*\right]\cos 2\theta\right\} \tag{4.1}$$

$$a_0^* = \frac{C^*F^*(1-u)}{C^*+F^*+C^*F^*(1-u)} \tag{4.2}$$

$$a_2^* = \beta b_2^* \tag{4.3}$$

$$\beta = \frac{(6+F^*)C^*(1-u)+2F^*u}{3F^*+3C^*+2C^*F^*(1-u)} \tag{4.4}$$

$$C^* = \frac{ER(1-u_s^2)}{E_sA_s(1-u^2)} \tag{4.5}$$

$$F^* = \frac{ER^3(1-u_s^2)}{E_sI_s(1-u^2)} \tag{4.6}$$

T is the axial force of the tunnel lining structure; P is the vertical stress; R is the tunnel radius; K is the ratio of the vertical stress to the horizontal stress; θ is the tunnel angle; a_0^* and b_0^* are dimensionless coefficients; C^* and F^* are the compressibility and flexibility, respectively;

E and E_S are the elastic moduli of the rock mass/soil mass and the support system, respectively; u and u_s are the Poisson's ratios of the rock mass/soil mass and the lining structure, respectively; A_S are the cross-sectional areas of the tunnel support; and I_S the moment of inertia of the tunnel support per unit length.

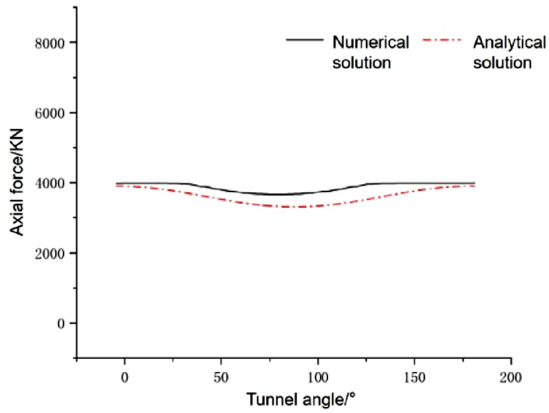

Fig. 4. Diagram of the circumferential inward force of the tunnel

In the calculation, it was assumed that the vertical stress of the soil mass inside the fault was constant and affected by the rock mass at a depth of 450 m at the top of the tunnel. As shown in Fig. 4, the numerical solution for the axial force in the model is compared with the internal force of the tunnel support system obtained using the analytical solution. The numerical solution for the axial force of the tunnel vault was 3690 kN, and the maximum analytical solution was 3290 kN. The axial force trend in the numerical model was the same as that in the analytical solution, and the error was controlled at 15%. The analytical solution fitted well with the numerical model, proving its accuracy and reliability of the numerical model.

5. Analysis of the stability of the support of the tunnel through the fault fracture zone

5.1. Initial in-situ stress

Figure 5 shows the initial in-situ stress state of Lianfeng Mountain. As shown in the figure, the displacement and stress of the mountain increase with an increase in depth under the action of self-weight stress after excavation because the rock in the fracture zone is relatively fragmented and scattered. When the external stress acts in this area, the area is more prone to stress redistribution than the surrounding area; therefore, the strain at the fault fracture zone is larger, and the stress is smaller.

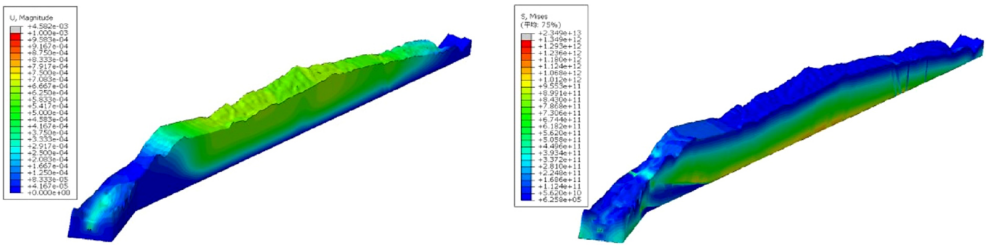

(a) (b)

Fig. 5. Initial in-situ stress state of Lianfeng Mountain: (a) Strain distribution contour; (b) Stress contour

5.2. Stability analysis of surrounding rock

To explore the stress distribution in the fracture zone, representative sections A, B, and C were considered for this area, and the azimuth map of the section is shown in Figure 6.

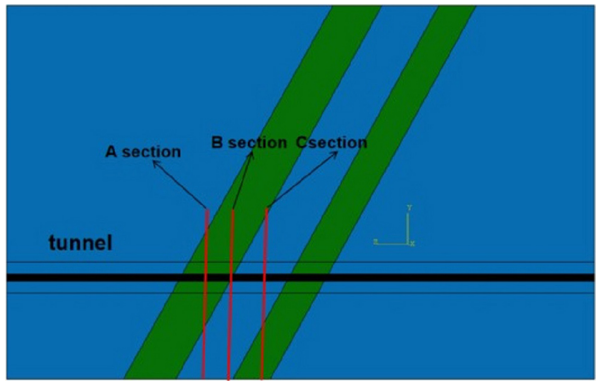

Fig. 6. Schematic diagram of a typical cross-section

5.2.1. Stress distribution law

1. Overall cloud map

To obtain the stress distribution law of the rock surrounding the mountain in the fracture zone, an excavation stress contour diagram of the mountain tunnel with a steel frame interval of 1m is shown in Figure 7. From the stress contour diagram, it can be observed that the stress distribution of the mountain is generally distributed with gravity, and it can be observed that the stress at the fracture zone is smaller than that of the intact area. From the analysis, it can be observed that the intact rock layer can bear greater stress due to its high strength and rigidity, and the constraint from the surrounding rock mass in the fracture zone area is small. The tunnel excavation will further reduce the restraint effect of the surrounding rock mass as it leads to the equilibrium deformation of the fracture zone and the release of stress.

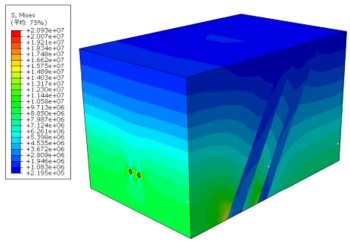

Fig. 7. Stress contour of mountain tunnel excavation

2. Cross-sectional contour

Figure 8 shows the stress contours of a typical tunnel cross-section. As shown in Figure 8(b) that the stress of the surrounding rock of the tunnel in the intact area is about 17.1 MPa, whereas the stress of the surrounding rock in the fracture zone of the same horizontal plane is 6.8 MPa, and the stress difference reaches 10.3 MPa. Through analysis, it can be observed that the tunnel excavation and support exert greater stress on the surrounding rock, whereas the strength of the soft rock at the junction of the soft and hard rock layers is lower and the deformation is larger; thus, the stress difference of the surrounding rock is much greater than that of the unexcavated rock mass.

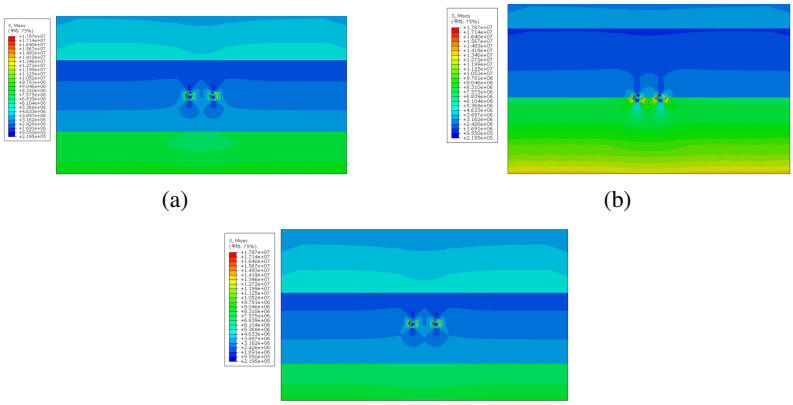

(a) (b)

(c)

Fig. 8. Stress contours of each section of the tunnel sections: (a) A; (b) B; (c) C

5.2.2. Strain distribution law

A strain cloud diagram of the mountain tunnel excavation with a steel frame interval of 1 m is shown in Figure 9. It can be observed that the plastic strain of the rock mass above and below the tunnel is large. The strain influence of the tunnel excavation area extends to the surface of the mountain, which is mainly manifested as the settlement of the mountain. The overall settlement above the tunnel is approximately 0.6 mm, and the settlement in the fracture zone area is slightly larger than that in the complete area.

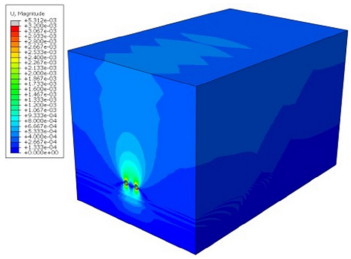

Fig. 9. Strain cloud diagram of mountain tunnel excavation

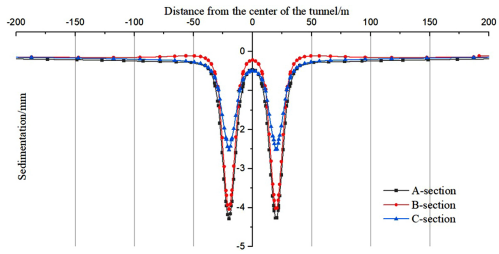

Fig. 10. Settlement curve of mountain cross-section

Take the cross-sectional settlement data 1m above the tunnel of the A, B, and C sections and make the curve as shown in Figure 10. It can be observed that the cross-sectional settlement curve of the mountain (W) is along the center of the tunnel in section A, the settlement of the top of the tunnel and the center of the two tunnels is 4.7 mm and 0.5 mm, respectively, and the settlement of the center of the tunnel above and the center of the two tunnels in section C is 2.6 mm and 0.5 mm, respectively, which shows that the degree of rock mass fragmentation has little influence on the deformation of the bunker between the two tunnels.

5.3. Stability analysis of tunnel steel frame lining

5.3.1. Stress distribution law

1. Steel frame lining

The stress contours of steel frames with different arrangement intervals are shown in Figure 11. As shown in Figs. 11(a)(b) and (c), the stress of the steel frame decreases with the decrease of the spacing of the steel frame, the stress of the steel frame decreases by 5% for every 100% increase in the number of steel frames, the stress on the inner steel frame is greater than that on the outer steel frame, and the stress on the inner side is approximately 20% greater than that on the outer side, which is more obvious in the fracture zone. After the analysis, it can be observed that when the vertical load of the mountain is transferred to the concrete lining structure, the inner side is subjected to greater stress when the load is received owing to the small area and volume of the inner side of the concrete lining structure. In an actual project, the strength of the inner steel frame should be increased to prevent stress failure on the inner side of the concrete lining.

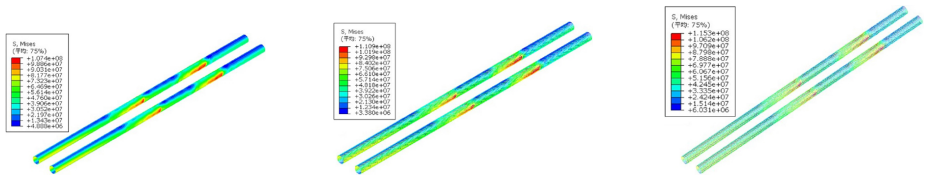

(a) (b) (c)

Fig. 11. Stress contour of steel frame: (a) 0.5 m interval; (b) 1.0 m interval; (c) 2.0 m interval

2. Concrete lining

The stress contours of the tunnel through the critical section of the fracture zone are shown in Figure 12. It can be observed that the stress distribution law of concrete lining structure is similar to that of steel frame, and the stress increases in the crushing zone; however, its stress magnitude is only 20% of the stress of steel frame. The stress of the surrounding rock on both sides of the tunnel is larger, and the stress magnitude gradually decreases with the tunnel wall from the inside to the outside. The maximum stress is 20.9 MPa, which is less than the maximum compressive standard value of C30 concrete. It can be observed that the stress of the lining structure is in a safe range.

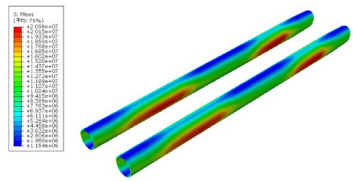

Fig. 12. Stress contour of tunnel fracture zone

5.3.2. Strain distribution law

1. Circumferential deformation law

Figure 13 shows the strain contours of the tunnel passing through the critical section of the fracture zone. It can be observed from the figure that the concrete lining structure has an obvious yield in the fracture zone owing to the inability to maintain self-stability after the stress release of the fault fracture zone. The convex deformation caused by the conduction to the lining structure and the settlement difference at the junction between the fracture zone and the complete rock mass is large, which can reach a maximum of 3 mm and may cause tensile or shear failure of the adjacent lining structure.

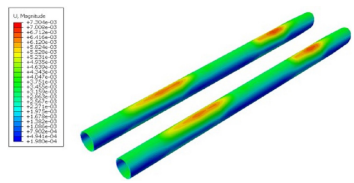

Fig. 13. Strain contour diagram of the tunnel fracture zone

Fig. 14 shows the polar coordinate diagram of the circumferential deformation of the tunnel with different sections and steel frame densities, which shows that the additional arrangement of the steel frame can effectively reduce the maximum deformation of the concrete lining structure. The maximum circumferential deformation of the basalt section decreases by 8.8%, 6.0%, and 3.2% with an increase in the density of the steel frame, and the maximum circumferential deformation of the breccia section decreases by 12.3%, 12.7%, and 8.0%, respectively. It can be observed that the steel frame has a better supporting effect in the crushing section. The settlement of the tunnel vault in the crushing section is much greater than the uplift at the bottom of the tunnel, which is because the tectonic breccia is more broken, and the rock mass has worse support performance for the tunnel at the vault position, which is more likely to lead to the settlement of the vault. The deformation of the left and right sides of the tunnel in the crushing section increases slightly after the laying of steel bars, and the increase is about 0.2 mm, which shows that the concrete lining structure in the crushing area bears a large vertical in-situ stress and is concentrated in the vault, and the stress can be effectively dispersed by adding the steel frame to avoid the tensile or compression failure of the concrete structure.

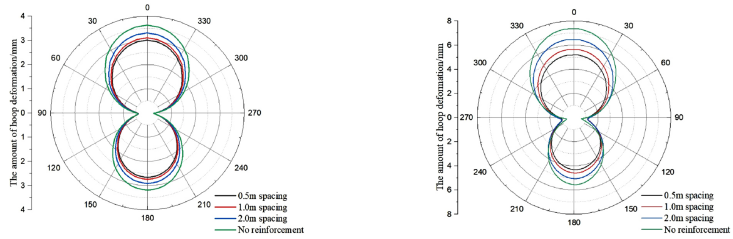

(a) (b)

Fig. 14. Polar diagram of tunnel circumferential deformation: (a) Basalt Interval; (b) Brecciate Section

2. Longitudinal deformation law

To explore the longitudinal deformation of the mountain at different vault angles, a longitudinal deformation diagram of the tunnel with a steel frame density in different sections is shown in Figure 15. It can be observed from Figure 15(b) that the bottom of the tunnel produces a bulge contrary to the distribution law of the tunnel vault, and when the rock mass is excavated, the rock mass undergoes a certain degree of elastic deformation, releasing the original stress, and the rock mass may have some elastic retraction, resulting in the bottom uplift. Figure 15(c) shows that the deformation on both sides of the tunnel is small, when there is no reinforcement, the deformation direction of the basalt section is perpendicular to the tunnel inward, the size is about 0.2 mm, the deformation direction of the broken section is perpendicular to the tunnel outward, the maximum deformation is 0.4 mm, and the vertical in-situ stress after the excavation of the basalt section is small. The two sides of the tunnel undergo slight deformation under the action of horizontal in-situ stress, and the vertical in-situ stress of the fracture zone is much greater than the horizontal in-situ stress, which causes the concrete structure on both sides to extrude outward, resulting in deformation in the opposite direction. The overall deformation of concrete can be effectively reduced by laying the steel frame, thereby reducing the lateral deformation caused by excessive deformation of concrete.

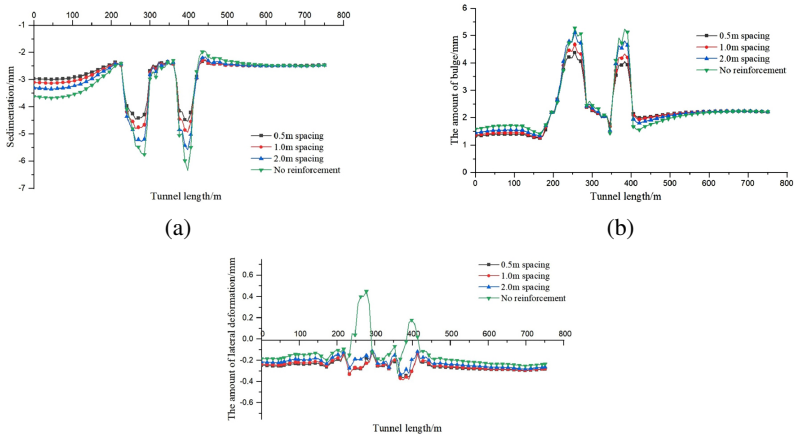

Fig. 15. Longitudinal cross-sectional deformation curves of the tunnel at different angles: (a) Vault settlement; (b) Deformation at the bottom; (c) Side deformation

Figures 15(a), (b) and (c) show that the settlement of the basalt mountain section at 0–200 m of the tunnel is greater than that of the basalt section of 400–800 m, and it can be observed that the steel frame can effectively reduce the vault settlement of the section because the section is located above the oblique fracture zone. After the tunnel excavation, the stress below the fracture zone is redistributed, resulting in an overall small-scale deformation of the rock mass of the fracture zone, subsequently affecting the complete rock layer above and causing additional settlement. The targeted arrangement of the steel frame in the above two sections can effectively control this phenomenon.

5.4. Settlement analysis during excavation

In double tunnel construction, the excavation of the second tunnel is performed after the first tunnel excavation is completed. To explore the mountain settlement law of this construction process, cross-sections A and B are taken in steps 3 and 5, respectively, to obtain the settlement curve, as shown in Figure 16.

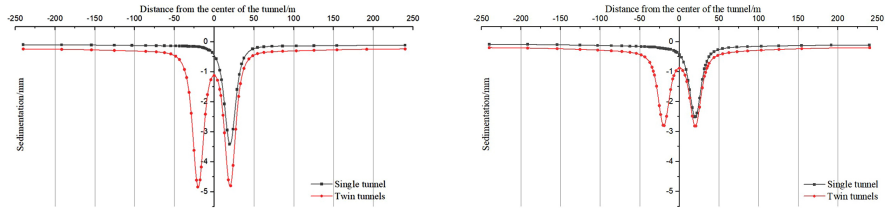

Fig. 16. Comparison curves of settlement in single and double tunnels: (a) Crushing area; (b) Intact area

Figures 16(a) and (b) show the settlement of the top of the tunnel under each construction condition. The top settlement of the single tunnel excavation in the crushing area is 3.41 mm, and the settlement increases to 4.79 mm after the excavation of the second tunnel, the increase is 40.5%. The settlement of the single tunnel excavation in the complete area is 2.51 mm, and the settlement of the second tunnel excavation is 2.86 mm, the increase is 13.9% For the rock mass on both sides of the tunnel, the settlement amount increases from 0.1 mm to 0.2 mm after single tunnel excavation and double tunnel excavation, that is, the influence of the second tunnel excavation on the rock mass outside the excavation area is uniformly increased by settlement, and the increase is approximately twice3-1 that of single tunnel settlement.

6. Conclusions

Because of the deformation law of the surrounding rock of the tunnel crossing the fault fracture zone under the action of deep buried high geostress, relying on the Lianfeng Tunnel crossing fault fracture zone project of Dayong Expressway in Yunnan Province, the numerical calculation and analysis method is used to study the stability characteristics of the tunnel crossing fault fracture zone under the action of high geostress. The main research conclusions are as follows:

1. The stress and strain of the tunnel support structure when crossing the crushing zone are greater than those of the complete area, and the settlement of the tunnel vault can be effectively reduced by the steel frame support; with an increase in the density of the steel frame, the return of the support effect decreases. From the analysis of this study, the most reasonable density of the steel frame is 1 m.
2. The stress on the inner side of the steel frame of the concrete lining structure was larger and more significant in the fracture zone, which was approximately 20% higher than that of the normal section. Therefore, it is recommended to enhance the strength of the inner steel frame in an actual project to prevent inner stress failure of the concrete lining structure.
3. The rock mass of the tunnel vault has poor support performance, and the settlement of the tunnel vault in the broken section is large. In an actual project, the support design of the vault area should be strengthened.
4. Owing to the stress redistribution caused by the slight deformation of the rock mass in the fracture zone, the vault produced additional settlement after the tunnel was excavated above the oblique fracture zone. This phenomenon can be effectively controlled by setting up the steel frames in these two sections in a targeted manner.
5. In the construction of adjacent double tunnels, the excavation of the second tunnel will cause a certain increase in settlement, in which the settlement increase of the rock mass fracture zone is larger, reaching 140% of the construction of the first tunnel. Therefore, in the design and construction stage, the engineer needs to fully explore the location, nature, and deformation characteristics of the weak layer and the fracture zone and provide appropriate support to reduce the settlement and deformation of the weak layer.

Acknowledgements

This work was supported by the Yunnan Provincial Key R&D Program (202003AC10002) and the Yunnan Provincial Academician Ace Han Workstation Funding Project (202105AF150076).

References

[1] S. Hao, R. Fei, and J. Yu, "Mechanical characteristics of ultra-shallow buried high-speed railway tunnel in broken surrounding rock during construction", *Archives of Civil Engineering*, vol. 68, no. 3, pp. 645–659, 2022, doi: 10.24425/ace.2022.141908.

[2] K. Zhu, K. Zhang, X. Wu, and X. Chen, "Force analysis and treatments for Lidong tunnel of Renxin expressway crossing karst caves", *Archives of Civil Engineering*, vol. 70, no. 1, pp. 693–705, 2024, doi: 10.24425/ace.2024.148936.

[3] H. Yuan, "Numerical simulation of mountain deformation and stress induced by multi-tunnel excavation", *Modern Information Science and Technology*, vol. 18, no. 6, pp. 142–146, 2022.

[4] Y. Li, S. Wang, and W. Liu, "Analysis of the Formation Causes and Stability Prediction of the Surrounding Rock of a Tunnel Crossing the Fracture Zone of a Water-rich Faul", *Mining Research and Development*, vol. 43, no. 5, pp. 142–146, 2023.

[5] E. Ma, Y. Zhong, and J. Yu, "Structural failure analysis of fracture zone of tunnel proximal fault based on fracture mechanics", *Highway*, vol. 68, no. 8, pp. 375–382, 2023.

[6] L. Meng, Y. Huang, and T. Li, "Study on Classification Correction Method for Asymmetric Extrusion of High Geostress Layered Soft Rock Tunnel", *Chinese Journal of Rock Mechanics and Engineering*, vol. 1, art. no. 147, 2022.

[7] Y. Zhang, Z. Xu, Y. Xie, J. Qiu, T. Yang, and Y. Xie, "Sensitivity and settlement control analysis of surrounding rock of tunnel in fault fracture zone", *Science Technology and Engineering*, vol. 23, no. 8, pp. 3493–3501, 2023.

[8] L. Chen, Y. Wang, Z.F. Wang, F. Fan, and Y. Liu, "Characteristics and treatment measures of tunnel collapse in fault fracture zone during rainfall: A case study", *Engineering Failure Analysis*, vol. 145, art. no. 107002, 2023, doi: 10.1016/j.engfailanal.2022.107002.

[9] Z. Zhang, H. Liu, H. Chen, S. Tan, and X. Tong, "Study on supporting technology of a mining roadway in fault fracture zone with high altitude", *Geotechnical and Geological Engineering*, vol. 41, no. 3, pp. 1839–1854, 2023, doi: 10.1007/s10706-022-02375-4.

[10] Y. Zheng, K. Wu, Y. Jiang, R. Chen, and J. Duan, "Optimization and design of pre-reinforcement for a subsea tunnel crossing a fault fracture zone", *Marine Georesources & Geotechnology*, vol. 41, no. 1, pp. 36–53, 2023, doi: 10.1080/1064119X.2021.2009602.

[11] Z. Li, "Inversion study on surrounding rock parameters in fault fracture zone of high-speed railway tunnel", *Journal of Shijiazhuang Tiedao University (Natural Science Edition)*, vol. 35, no. 4, pp. 53–59, 2022.

[12] Q. Tao, "Study on stability control of soft rock tunnel with high geostress considering swelling effect of rock mass - Taking Milin tunnel as an example", *Tunnel Construction (in Chinese and English)*, vol. 43, no. 8, pp. 1327–1337, 2023.

[13] H. Zhe and Z. Tao, "In-situ stress distribution in different rocks", *Acta Seismologica Sinica*, no. 1, pp. 49–63, 1994.

[14] M. Shen and J. Chen, *Rock mass mechanics*. Shanghai: Tongji University Press, 2015.

Received: 2024-05-30, Revised: 2024-07-30